Chapter 3

Reactive Compatibilized Poly (2,6-dimethyl-1,4-phenyl ether) and Polyamide-6,6 Blends with the addition of low molecular weight Poly (2,6-dimethyl-1,4-phenyl ether)

Abstract

A low molecular weight poly (2,6-dimethyl-1,4-phenyl ether) (lmw PPE), possess high hydroxyl end group concentration has been used to increase the functionality of the PPE component in the immiscible Polyamide-6,6 (PA-6,6) and PPE blend. In addition, a bi-functional epoxy monomer able to react with both the functional end groups of PA-6,6 and PPE was introduced into the blend. The low molecular PPE has better mobility to migrate to the interface to react with PA-6,6, and more in situ formed copolymers can be expected, compared to the high molecular weight PPE. Therefore, better compatibilization effect was achieved, as shown by the reduced domain size and improved mechanical properties.

3.1 Introduction

Polymer blends of Poly (2,6-dimethyl-1,4-phenyl ether) (PPE) and polyamide-6,6

(PA-6,6) is probably the best example of a blend composed of an amorphous and a

semi-crystalline polymer. PPE is a unique polymer with some distinct advantages,

such as high rigidity, high glass transition temperature, high heat resistance and good

dimensional stability; however, it has very poor processibility as well as chemical

resistance [1]. On the other hand, PA-6,6 offers good processibility and chemical

resistance, but lack of dimensional stability and readily absorb water [2]. The

combination of high heat resistance, good processibility, dimensional stability and

chemical resistance of PA-6,6/PPE blends has encouraged large scale of commercial

development of these materials. Under the trade name Noryl GTX of GE Plastics, it

has enjoyed great success in various industrial applications, especially in the

automotive segment, which requires high heat resistance for the on-line painting

process, good dimensional stability and low CLTE [3].

Due to the thermodynamic incompatibility of PA-6,6 and PPE, compatibilization

is required to develop the appropriate morphology and sufficient interface adhesion to

obtain a useful blends with synergistic properties. Numerous compatibilization

strategies have been discussed in the literatures and patents by several workers [4-22].

Most of these methods involve the grafting of a functional group (e.g., maleic

anhydride, fumaric acid, citric acid, etc.) to the PPE chain that will react with the amine end groups of the polyamide. The introduction of a compatibilizer precursor that is miscible with the PPE phase and that reacts with the polyamide phase has also been used effectively to compatibilize this system [13,14,16]. In addition, the coupling type reactive compatibilization approach has been successfully applied to deliver PA-6,6/PPE blends with satisfactory mechanical properties [15,20,21].

In this study, an ultra low molecular weight PPE (lmw PPE), recently launched by GE plastics by redistribution (de-polymerization) of high molecular weight PPE with tetramethyl substituted bisphenols, and tetramethyldiphenoquinone (TMDPQ) as catalyst [23-25], is employed in the reactive compatibilized Nylon-6,6/PPE blends. Comparing to the conventional commercial available high molecular weight PPE, the low molecular weight PPE possess higher hydroxyl end group contents (Table 3-1), which means more reaction site for reactive compatbilization; and lower viscosity for better processability. Additionally, an low molecular weight bi-functional epoxy coupler, which is able to react with both the functional end groups of PPE and nylon-6,6, is incorporated into the system (Scheme 3-1). It is expected that with the higher contents of hydroxyl end group of the low molecular PPE, greater amount of in situ formed PPE-co-epoxy-co-PA-6,6 copolymers will be generated. Consequently, the number of effective in situ formed copolymers, acting as compatibilizers will be

increased, which in turn give polymer blends with reduced interfacial tension and

improved mechanical properties. The relaxation behavior, morphology and

mechanical properties of the reactive compatibilized PA-6,6 /PPE blends will be

discussed.

3.2 Experimental

3.2.1 Materials

Polyamide-6,6, Zytel 101L, was obtained from DuPont Engineering Polymer. High molecular weight PPE, Blendex HPP820, and a low molecular weight PPE, Blendex HPP857 (now under the tradename of PPO SA120 of GE Plastics) were purchased from GE Specialty Chemicals. The bi-functional epoxy resin, Epon 828 was supplied by Shell Chemical Company. Table 3-1 and Table 3-2 list the properties and the chemical structures of materials used in this work, respectively. All materials were used as received.

3.2.2 Extrusion and injection molding

All blends were dry mixed first and the melt blending process was carried out with a 30-mm co-rotating intermeshing twin-screw extruder (L/D=42, Kobe Steel Co., Japan) with a rotational speed 200 rpm. Figure 3-1 presents the screw configuration used in preparing the polymer blends. The standard ASTM test specimens were prepared by an Arburg 3oz injection-molding machine. Prior to melt blending and injection molding, all pellets/powder were dried in an oven at 80℃ for 4 hours. The detailed processing conditions for extrusion and injection molding are summarized in Table 3-3.

3.2.3 Dynamic mechanical analysis measurements

Dynamic mechanical analysis (DMA) measurements were carried out in order to analyze the phase behavior of the blends. The DMA measurements were done in the bending mode with a frequency of 1 Hz and a heating rate of $2°C$/min by Perkin Elmer DMA 7. The ASTM standard Izod impact test specimens were used to perform the DMA measurements. To avoid the effect of moisture contents on the glass transition temperature (α relaxation) of Polyamide [26,27], all the test specimens were dried in a dehumidified dryer at $80°C$ for 4 hours.

3.2.4 Scanning electron microscopies

The morphologies were examined by a Scanning Electron Microscopy (SEM) at accelerating voltage 20 kV, Model S-570, Hitachi Co. of Japan from cryogenically fractured specimens in the plane perpendicular to flow direction of injection molding. Samples were etched with chlorform to dissolve the PPE phase out of the blends. The fractured surfaces of specimens were coated with thin film of gold to prevent charging.

3.2.5 Mechanical properties

An Instron Universal Testing Machine model 4201 was used to measure the

mechanical properties of the uncompatibilized and compatibilized blends. Tensile

tests were measured according to the ASTM D638 method with crosshead speed

5mm/min at ambient conditions. Flexural tests were measured according to ASTM

D790 method with 50mm span and 5mm/min test speed at ambient condition.

Unnotched Izod impact test were done at ambient temperature according to ASTM

D256 method.

3.3 Results and discussion

3.3.1 Relaxation behavior

The relaxation behavior of polymer blends is an important indication for intermolecular interactions and thus for polymer/polymer miscibility of the amorphous regions. Strong changes of the segment motion can be induced by the thermodynamic miscibility in polymer blends [40]. This behavior is reflected by the occurrence of single composition dependent glass transition temperature T_g in miscible blends. In the case of partial miscible blends, the glass transition temperature remains separated but the T_gs are shifted in comparison to the T_gs of the pure components toward each other. In completely immiscible polymer blends the T_gs are unaltered.

The glass transition temperature of the incompatibilized and compatibilized PA-6,6/PPE blends were determined by the loss factor tanδ of DMA and shown in Table 3-4. In the PA-6,6/PPE=50/50 blend, the glass transition temperature of PA-6,6 and PPE are 72℃ and 210℃, respectively. This corresponds to the value of neat dry nylon-6,6 and PPE, respectively [26]. The unchanged T_gs implies that the PA-6,6/PPE=50/50 blend is completely immiscible. In the blend of PA-6,6/PPE/Epon828 = 50/50/1phr, the T_g of PA-6,6 and PPE has shifted to 79℃ and 208℃, respectively. The significant T_g increase of PA-6,6 is due to the molecular

weight increase of PA-6,6, caused by the chain branching, extension and crosslinking reactions between PA-6,6 and Epon828 (Scheme 3-1). The small T_g shift of PPE to lower temperature may be originated from the following two reasons. Firstly, it is exploited in recent studies that PPE is miscible with low molecular epoxy [28-32]. As a result, Epon828 may function as a plasticizer here and decreases the T_g of the PPE phase. Secondly, portions of the in situ formed PPE-co-epoxy-co-PA-6,6 copolymers acts as compatibilizers [15], which in turn improve the miscibility between PPE and PA-6,6 and thus small T_g shift of the PPE phase.

In the cases where 20wt% of the high molecular weight PPE is replaced by the low molecular weight PPE, the relaxation behaviors are somewhat different. The glass transition temperature of the PPE phase in the PA-6,6/PPE/lmw PPE = 50/30/20 blend drops from 210℃ to 188.5℃, which is very close to the predicted theoretical value of 187℃ determined by the Fox law [33]. The exhibited single T_g indicates the low molecular weight PPE is completely miscible with the high molecular weight PPE. In the PA-6,6 phase, the T_g remains unchanged, implying that the low molecular weight PPE prefers to stay in the PPE phase, and has not caused any plasticizer effect to the PA-6,6 phase. When Epon828 has been added to the blends (PA-6,6/PPE/lmwPPE/Epon828 = 50/30/20/1phr), the T_gs of PA-6,6 phase and PPE phase have been shifted from 72℃ to 75℃ and 188.5℃ to 185℃, respectively. The

small T_g shift of the PPE phase can be again attributed to the improved compatibility between PPE and PA-6,6 as well as the plasticizing effect of Epon828 on the PPE phase. Comparing the extent of T_g shift of PA-6,6 in PA-6,6/PPE/Epon828 = 50/50/1phr (7℃) with that of PA-6,6/PPE/lmwPPE/Epon828 = 50/30/20/1phr (3℃), it is obvious that the chain branching, extension or crosslinking of PA-6,6 is significantly reduced in the existence of the low molecular weight PPE.

Based on the above findings, the following compatibilization mechanism (Scheme 3-2) is proposed for the PA-6,6/PPE reactive compatibilized blends. For the compatibilized blend (PA-6,6/PPE/lmwPPE/Epon828 = 50/30/20/1phr), during the extrusion process the PPE powder melt first (table1), and the Epon 828 will preferentially reside in the melt PPE phase. Due to the higher hydroxyl end group contents in the low molecular weight PPE than that of high molecular PPE (425 μ mol/g VS. 80 μ mol/g), the former has more opportunity to react with Epon828. Subsequently when the PA-6,6 pellets are melted, the low molecular weight PPE coupled with Epon828 has better mobility to migrate to the interface [43], and further react with the PA-6,6 functional end groups to form various PPE-co-epoxy-co-PA-6,6 copolymers to function as effective compatibilizers. The residual un-reacted Epon828 may further react with PA-6,6, and results in the branching, chain extended or crosslinked PA-6,6, which in turn causes the T_g increase of the PA-6,6 phase. Since

the extent of T_g increase of the PA-6,6 phase is moderate, it can be speculated that

Epon828 was evenly consumed by both PPE phase and PA-6,6 phase. In contrast, if

the low molecular weight PPE is not introduced in the blend (PA-6,6/PPE/Epon828 =

50/50/1phr), only very small portion of the Epon828 react with the high molecular

weight PPE, due to its low hydroxyl contents. In fact, most of the Epon828 was

consumed by the PA-6,6, as evidenced by the significant T_g increase of the PA-6,6

phase in the PA-6,6/PPE/Epon828=50/50/1phr blend. The compatibilzation

mechanism will be further examined in the morphology and mechanical properties
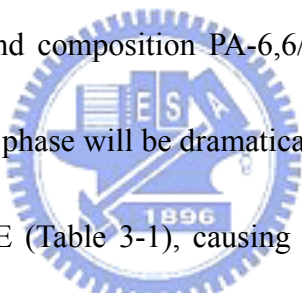
sections.

3.3.2 Morphology

3.3.2.1 Effect of viscosity ratio and interfacial tension

The morphology development in polymer blends is controlled by the deformation,

breakup and coalescence of the dispersed phase (domain) [34-36]. The flow field

provided by the mixing equipment, e.g. twin screw extruder, generates viscous shear

force to break the dispersed phase into small domains. At the same time, the flow field

also provides collision opportunity between domains and cause coalescence. The

interfacial tension between two polymers provides a thermodynamic driving force to

resist domain deformation and favor coalescence. In polymer blends, the breakup and

deformation of the dispersed phase is mainly governed by the capillary number, Ca, the ratio of the shear stress τ exerted on the dispersed phase by the external flow field and the interfacial stress σ/R, where σ is the interfacial tension and R the local radius of the dispersed phase: $Ca = \tau R/\sigma$ [36]. Above a critical value, Ca_{crit}, the viscous shear stress overrules the interfacial stress and the dispersed phase will break up into smaller droplets. The critical capillary number, Ca_{crit}, depends on both the viscosity ratio between the dispersed phase and the continuous phase, $P = \dfrac{\eta_d}{\eta_m}$, and the type of flow. Wu [37] has conducted a systematic study on the formation of dispersed phase in incompatible polymer blends. He found that the Weber number appears to have the lowest value when the viscosity ratio $P = \dfrac{\eta_d}{\eta_m}$ closely equals to one, which means the smallest average domain size will be obtained. As the viscosity ratio increases above unity or decreases below unity, the dispersed particles become larger. Furthermore, the domain size reduction easily occurs when the interfacial tension σ between of the two polymer melt is lower, even if considerable melt viscosity difference is existed. In general, it is easier to obtain finer domain size under conditions where the two melt viscosities are close, or with low interfacial tension between each polymer melt.

The SEM pictures of the various PA-6,6/PPE blends are shown in Figure 3-2 and Figure 3-3. The domain size for both PA-6,6/PPE/Epon828 = 50/50/1phr and

PA-6,6/PPE/lmw PPE = 50/30/20 are much finer than that of PA-6,6/PPE=50/50. The

viscosity ratio of PA-6,6/PPE=50/50 can be roughly estimated from Table 1. The

extremely large viscosity ratio implies that it should be very difficult to break up the

dispersed phase into small domains. In PA-6,6/PPE/Epon828 = 50/50/1phr, the

viscosity of PA-6,6 will be prominently increased, due to the occurrence of the

branched, chain extended and crosslinked PA-6,6, manifested by the significant T_g

increase in the DMA measurement. Therefore, the viscosity ratio λ of

PA-6,6/PPE/Epon828 = 50/50/1phr will be much closer to one than that of

PA-6,6/PPE = 50/50. For blend composition PA-6,6/PPE/lmw PPE = 50/30/20, the

viscosity of the dispersed PPE phase will be dramatically dropped with the addition of

the low molecular weight PPE (Table 3-1), causing the viscosity ratio shift to one.

Based on the general rule that the smaller domain size will be obtained with viscosity

ratio closer to unity, it can be predicted that both the domain size of

PA-6,6/PPE/Epon828 = 50/50/1phr and PA-6,6/PPE/lmw PPE = 50/30/20 blends will

be smaller than that of PA-6,6/PPE=50/50 blend. From the SEM results, it is found

that the trend of the domain size reduction predicted by Wu's conclusions [37] is in

good agreement with the experimental results. Therefore in designing polymer blends,

it is critical to take the viscosity ratio and interfacial tension between the two polymer

melts into consideration to control the morphology development.

3.3.2.2 Reactive compatibilized blend

The effectiveness of reactive compatibilization on the domain size reduction of immiscible polymer pairs has been reviewed in several books [35,41,42]. It is found that even small amounts of reactive in situ formed copolymer greatly reduce the interfacial tension between polymers. Sundararaj [38] used the breaking thread method to measure the interfacial tension of reactive blends of maleic anhydride functional EPDM rubber and amine functional polystyrene, and oxazoline functional polystyrene and polyamide. In each case, the measured interfacial tension of the reactive pair was approximately half of the similar non-reactive pair. Chapleau et al. [39] also used the breaking thread method to measure the interfacial tension between Polyethylene and Polyamide 6 in the presence of an ionomer comprised of ethylene, methacrylic acid and isobutyl acrylate. Blends compatibilized with 10 wt% ionomer had approximately half the interfacial tension of the uncompatibilized blends.

Figure 3-3(d) presents the SEM pictures of the PA-6,6/PPE/lmwPPE/Epon828 = 50/30/20/1phr blend. The finest domain size is obtained with this composition among the blends studied. This further proves the plausibility of the proposed compatibilization mechanism in the previous section. The low molecular weight PPE provides more reaction site to epoxy as well as better mobility to migrate to the interface. Therefore, more in situ formed copolymers are generated, and effectively

lower the interfacial tension, and thus finer domain size obtained.

3.3.3 Mechanical properties

The mechanical properties can be served as an indicator for the effectiveness of a

compatibilizer in immiscible or incompatible blends. Generally it is expected that the

mechanical properties of the compatibilized polymer blends will be improved

compared to the corresponding incompatibilized ones because of the lower interfacial

tension and enhanced interfacial adhesion of the compatibilized blends, making stress

transfer more efficiently between phases during fracture [13-15]. The SEM pictures of

the unnotched impact fractured test specimen at room temperature without solvent

etching of the dispersed PPE phase were shown in Figure 3-4. The distinct domain

seen in the PA-6,6/PPE = 50/50 blend [Figure 3-4(a)] indicates de-bonding the

interface is rather easy, due to the high interfacial tension and sharp interface of the

completely immiscibility between PA-6,6 and PPE. In the PA-6,6/PPE = 50/50/1phr

blend, the de-bonding become more difficult, as seen from the un pulled-out of the

PPE particles [Figure 3-4(b)]. This suggests the blend has been moderately

compatibilized. Examining the SEM picture of the compatibilized

PA-6,6/PPO/lmwPPO/Epon828 = 50/30/20/1phr blend [Figure 3-4(c)], it is interesting

to note that no distinct domains can be observed. The reduced interfacial tension and

broadened interface are responsible for such morphological change during fracture.

The tensile strength, flexural modulus and unnotched impact strength were given in figure 3-5. The degree of mechanical property improvements is in the following order: {[PA-6,6/PPO/lmwPPO/Epon828 = 50/30/20/1phr], (A)} > {[PA-6,6/PPE = 50/50/1phr], (B)} > {[PA-6,6/PPE/lmwPPO = 50/30/20], (C)} > {[PA-6,6/PPE = 50/50], (D)}. As discussed earlier, composition (A) is the best compatibilized, and the reduced interfacial tension and broader interfaces will make stress transfer more efficiently between phases during fracture. Consequently, the best mechanical properties improvements are obtained from composition (A). Composition (B) ranks number 2 in the mechanical properties improvements, although from the SEM pictures (Figure 3-3) its domain size is very close to composition (C). It is because in composition (B), except been moderately compatibilized, certain portions of the PA-6,6 are branched, chain extended or even crosslinked, resulting in higher molecular weight, and in turn gives higher mechanical strength. On the contrary, in composition (C) the strength of the PPE phase was inevitably decreased, due to the addition of low molecular weight PPE, while that of the PA-6,6 was unaffected. However, the mechanical properties of composition (C) are still better than that of composition (D), due to the coarse domains of the latter become intrinsic defects, and thus very poor mechanical properties.

3.4 Conclusions

The introduction of the low molecular weight PPE provide several advatange in preparing PA-6,6/PPE blend with satisfied properties. First of all, the ultra low viscosity of the low molecular weight PPE significantly altered the viscosity mismatch between PA-6,6 and PPE, and the domain size was reduced accordingly. Moreover, the high hydroxyl end group of the low molecular weight PPE provides additional reaction site to the epoxy coupler, compared to the high molecular weight PPE. Without the existence of the low molecular weight PPE, the epoxy coupler tends to react solely with PA-6,6, as shown by the increased PA-6,6 T_g. On the other hand, addition of the low molecular weight PPE enables the epoxy coupler to react evenly with both components in the blend. As a result, more in situ formed copolymers are generated. The fractured surface shows the bonding between the PA-6,6 and PPE was strengthened in the compatibilized blend. In addition, improvements in mechanical properties were also found in the compatibilized blend. The above results prove that addition of the low molecular weight PPE, along with the epoxy coupler, provide an alternative compatibilization approach for the immiscible PA-6,6/PPE blends.

Reference

1. J. A. Brydson, "Plastics Materials", 4th ed., Butterworthy Scientific, London (1982).

2. M. I. Kohan, Ed., "Nylon Plastics Handbook", Hanser, Munich (1995).

3. D. Wohrle, *Proc. Of the 21. Darmstadter Kunststoff-Kolloquium*, Sept. 2001.

4. J. R. Campbell, S. Y. Hobbs, T. J. Shea, and V. H. Watkins, *Polym. Eng. Sci.*, **30**, 1056 (1990).

5. S. Takayama and K Takeda, *Kobunshi Ronbunshu*, 50, 919 and 953 (1993).

6. M. K. Akkapeddi, B. V. Buskirk, and G. J. Dege, *Soc. Plast. Eng.*, **52**, 150 (1994).

7. M. Kakugo, T. Maruyama, H. Abe., Y. Suzuki, and T. Sanada, *Kagaku Kogaku*, **60(6)**, 15 (1996).

8. T. Hatashi, A. Watanabe, T. Hajime, and T. Nishi, *Kobunshi, Ronbunshu*, **49(4)**, 373 (1992).

9. S. Y. Hobbs, M. E. J. Dekkers, and R. V. H. Watkins, *J. Mater. Sci.*, **24**, 1316 and 2025 (1989).

10. K. Ueno and T. Maruyama, U.S. Patents 4,315,086 and 4,338,410, Sumitomo Chemical, 1982.

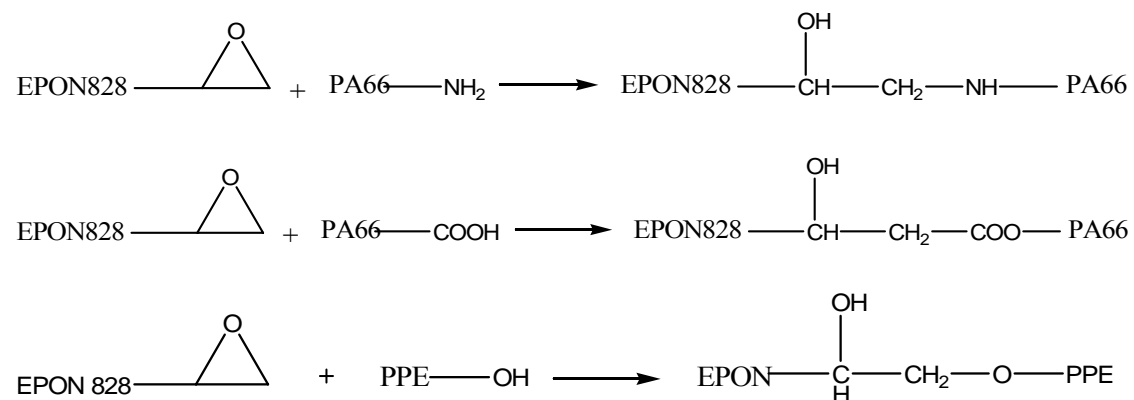11. G. F. Lee, J. M. H. Heuschen, and R. Van Der Meer, PCT Intl. Appl., WO

87/05311, General Electric, 1987.

12. M. K. Akkapeddi, B. V. Buskirk, and A. C. Brown, PCT Intl. Appl., WO 88/08433, Allied Signal, 1988.

13. C. R. Chiang and F. C. Chang, *J. Appl. Polym. Sci.*, **61**, 2411 (1996).

14. C. R. Chiang and F. C. Chang, *Polymer*, **38**, 3807 (1997).

15. C. R. Chiang and F. C. Chang, *J. Polym. Sci., Part B*, *Polym. Phys*., **36**, 1805 (1998).

16. H. Kasahara, K. Fukuda, and H. Suzuki, U.S. Patent 4,339,376, Asahi-Dow, 1983.

17. D. Ghidoni, E. Bencini, and R. Nocci, *J. Mater. Sci.*, **31**, 95 (1996).

18. S Fujii, H. Ishida, M. Morioka, A. Saito, and R. Van der Meer, U.S. Patent 4,873,276, General Electric, 1989.

19. T. Nishio, T. Sanada, and T. Okada, U.S. Patent 5,159,018, Sumitomo Chemical, 1992.

20. C. R. Chiang, C. R. Tseng, and F. C. Chang, *J. Polym. Res.*, **4**, 91 (1997).

21. C. R. Chaing, M. Y. Ju, and F. C. Chang, *Polym. Eng. Sci.*, **38**, 622 (1998).

22. H. A. M. Van Aert, G. J. M. Van Steenpaal, L. Nelissen, P. J. Lemstra, J. Liska, and C. Bailly, *Polyme*r, **42**, 2803 (2001)

23. H. A. M. Van Aert, M. H. P. Van Genderen, G. J. M. Van Steenpaal, L. Nelissen,

E. W. Meijer and J. Liska, *Macromolecules*, **30**, 6056 (1997).

24. J. Liska et al., U.S. Patent 5,880,221, 1999.

25. J. Krijgsman, J. Feijen, and R. J. Gaymans, *Polymer*, **44**, 7055 (2003).

26. H. W. Starkweather, Transitions and relaxations, in "Nylon Plastics Handbook", :
     M. I. Kohan, Ed., Hanser, Munich (1995).

27. A. Ishisaka, M. Kawagoe, *J. Appl. Polym. Sci.*, **93**, 560 (2004)

28. Y. Ishii, A. J. Ryan, *Macromolecules*, **33**, 158 (2000).

29. Y. Ishii, A. J. Ryan, *Macromolecules*, **33**, 167 (2000).

30. A. Saalbrink, A. Lorteije, and T. Peijs, *Composites Part A*, **29**, 1243 (1998).

31. R. Vanderbosch, M. E. H. Meijer, and P. J. Lemstra, *Polymer*, **35**, 4349 (1995).

32. Tracy et al., U.S. Patent 5,834,565, General Electric, 1998.

33. T. G. Fox, *Appl. Bull. Am. Phys. Soc.*, **1**, 123 (1956).

34. J. J. Elmendorp, in "Mixing in Polymer Processing", C. Rauwendaal, Ed.,
     Marcel Dekker, New York (1991).

35. C. E. Scott, and N. D. B. Lazo, in *"Reactive Polymer Blending"*, W. Baker, C.
     Scott, and G. H. Hu, Eds., Hanser, Munich (2001).

36. H. E. H. Meijer and J. M. H. Janssen, in *"Mixing and Compounding of
     Polymers"*, I. Manas-Zloczower and Z. Tadmor, Eds., Hanser, Munich (1994).

37. S. H. Wu, *Polym. Eng. Sci.*, **27**, 335 (1987).

38. U. Sundararaj, PhD Thesis, Univ. Minnesota (1994).

39. N. Chapleau, B. D. Favis, and P. J. Carreau, *J. Polym. Sci., Part B, Polym. Phys.*, **36**, 1947 (1998).

40. M. M. Coleman, J. F. Graf, and P. C. Painter, "Specific Interactions and the Miscibility of Polymer Blends", Technomic Publishing, Lancaster, PA, 1991.

41. P. S. Hope and M. J. Folkes, "Polymer Blends and Alloys", Chapman and Hall, 1993.

42. D. R. Paul and C. B. Bucknall, "Polymer Blends", John Wiley & Sons, New York, 2000.

43. J. Reiter, G. Zifferer and O. J. Olaj, Macromolecules, 23, 224 (1990).

Scheme 3-1. Chemical Reactions Involved in this Study

EPON828 —— (epoxide) + PA66—NH$_2$ → EPON828——CH(OH)——CH$_2$—NH——PA66

EPON828 —— (epoxide) + PA66—COOH → EPON828——CH(OH)——CH$_2$—COO——PA66

EPON 828 —— (epoxide) + PPE——OH → EPON——CH(OH)——CH$_2$—O——PPE

Scheme 3-2. Schematic Diagram of Compatibilization Mechanism

PA 6,6 + PPE + lmw PPE + EPON 828

↓

Extruder

↓ *Stage 1*

Unmelted PA 6,6 Pellet

+

EPON 828

PPE — OH — R

R — OH — PPE

↓ *Stage 2*

PA 6,6 — NH$_2$ — PPE
Branched PA 6,6

PA 6,6 — COOH — PPE
Crosslinked PA 6,6

PA 6,6 — OH — PPE
Chain extend PA 6,6

PPE
OH — PPE
PPE — OH
PPE

Sharp Interface

↓ *Stage 3*

PA 6,6 Phase   *PA 6,6-co-EPOXY-co-lmw PPE*   **PPE Phase**

Broad Interface
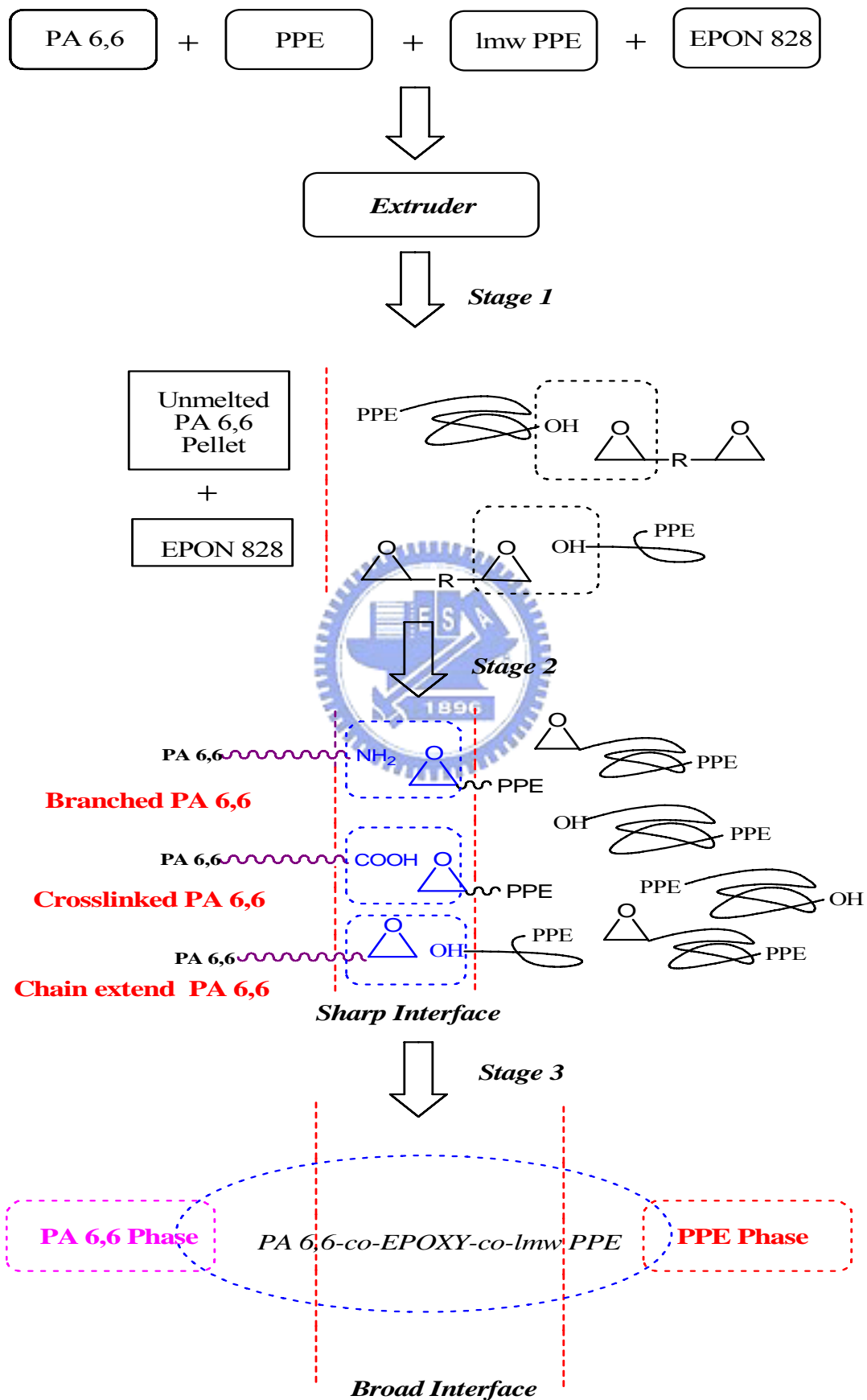
Table 3-1. Properties of Materials Used in the Study

Grade	Blendex HPP 820	Blendex HPP 857	Zytel 101L	Epon828
Appearance	Powder	Granule	Pellet	Liquid
Density(g/cm3)	1.02	1.02	1.06	1.16
Tg (℃)	215	160	73	
Tm(℃)			262	
Decomposition Temp(℃), TGA, N2	460	440		
Dielectric Constant	2.5	2.5		
Melt Viscosity(Pa.S)	100,000[a]	32[a]	100[b]	11~15[c]
Mw, GPC	60,000	6,300		
Mn, GPC	25,000	2,350		
Polydispersity Index	2.4	2.7		
Phenolic End Groups(μ mol/g), FTIR	80	425		
Epoxy Equivalency (g/eq)				185-192

(a) @260℃, 1 rad/sec (b) @280℃, shear rate 100s^{-1} (c) @25℃

Table 3-2. Chemical Structures of Materials Used in this Study

PA66

$$H_2N\left[\!\!\left(CH_2\right)_{\!6}\overset{H}{\underset{}{N}}-\overset{\displaystyle O}{\underset{}{C}}-\left(CH_2\right)_{\!4}\overset{\displaystyle O}{\underset{}{C}}\right]_{\!n}\!\!OH$$

PPE
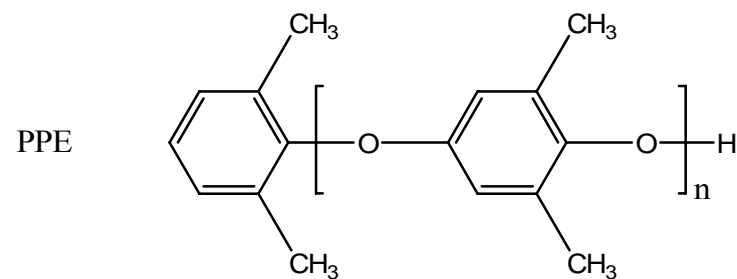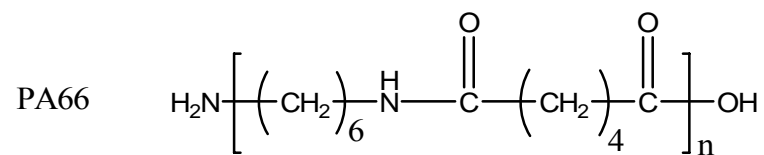
Epon828
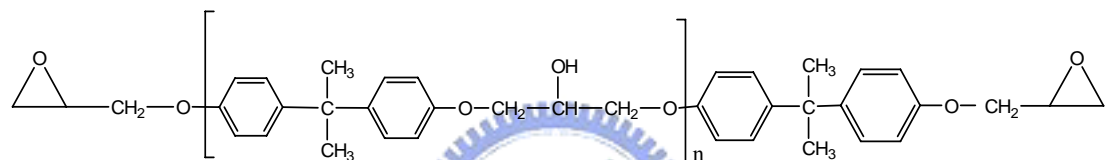
n=0.1

Table 3-3. Processing Conditions

| Temp (℃) | | | | | | | | | | | | | | | |
Stage	C0	C1	C2	C3	C4	C5	C6	C7	C8	C9	C10	C11	Die	Nozzle	Mold
Extrusion	220	240	260	280	290	295	290	285	295	295	285	285	285		
Injection	255	285	295	-	-	-	-	-	-	-	-	-	-	295	80

Table 3-4. T_gs of PA-6,6 and PPE in Various PA-6,6/PPE Blends Obtained from DMA Test

Blend Composition	PA-6,6 T_g	PPE T_g
PA-6,6/PPE = 50/50	72	210
PA-6,6/PPE/Epon828 = 50/50/1phr	79	208
PP-6,6/PPE/lmw PPE = 50/30/20	72	188.5
PP-6,6/PPE/lmw PPE/Epon828 = 50/30/20/1phr	74	185
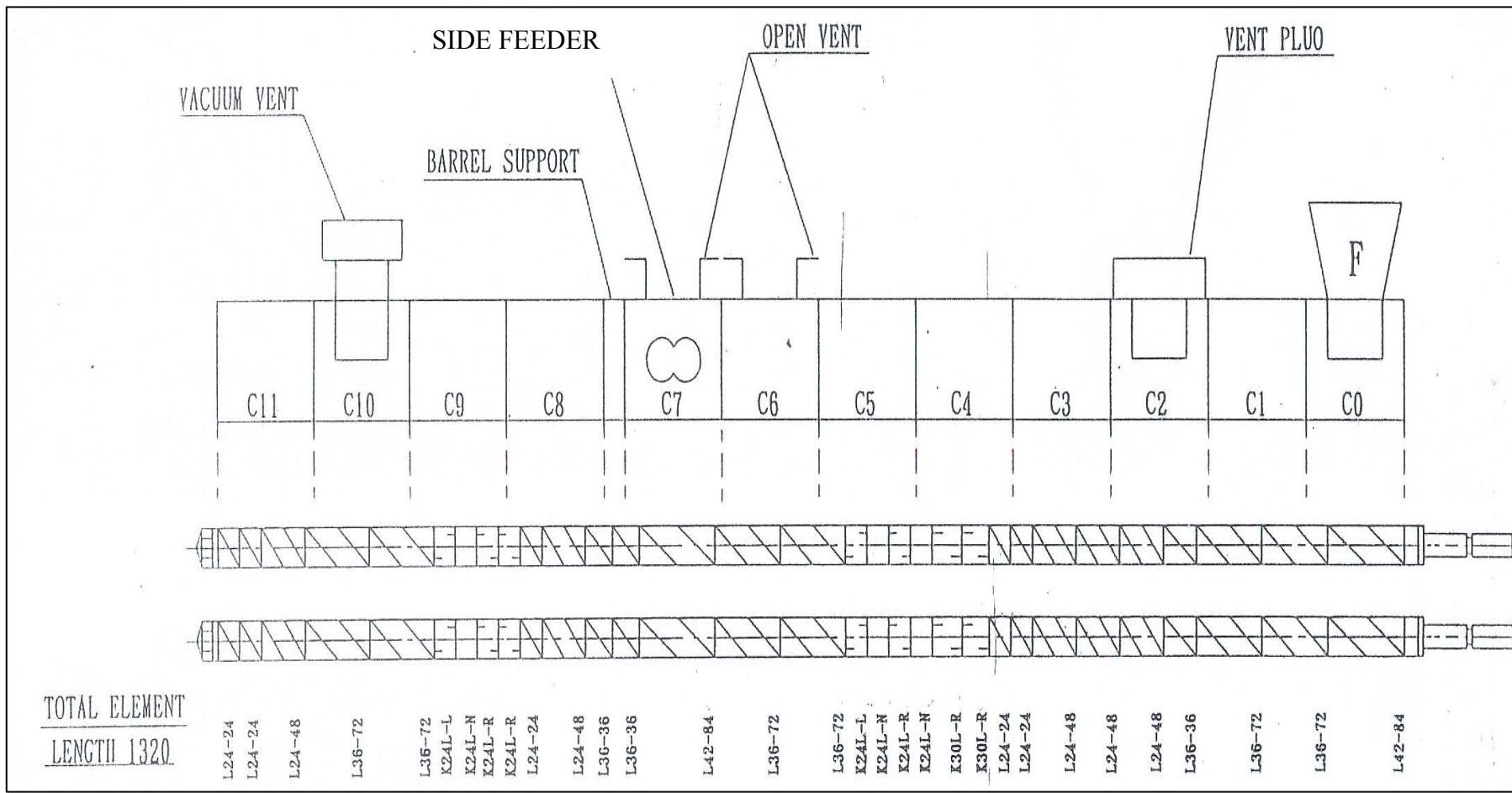
Figure 3-1. Screw configuration used in the twin screw extruder.

(a) (b) (c)
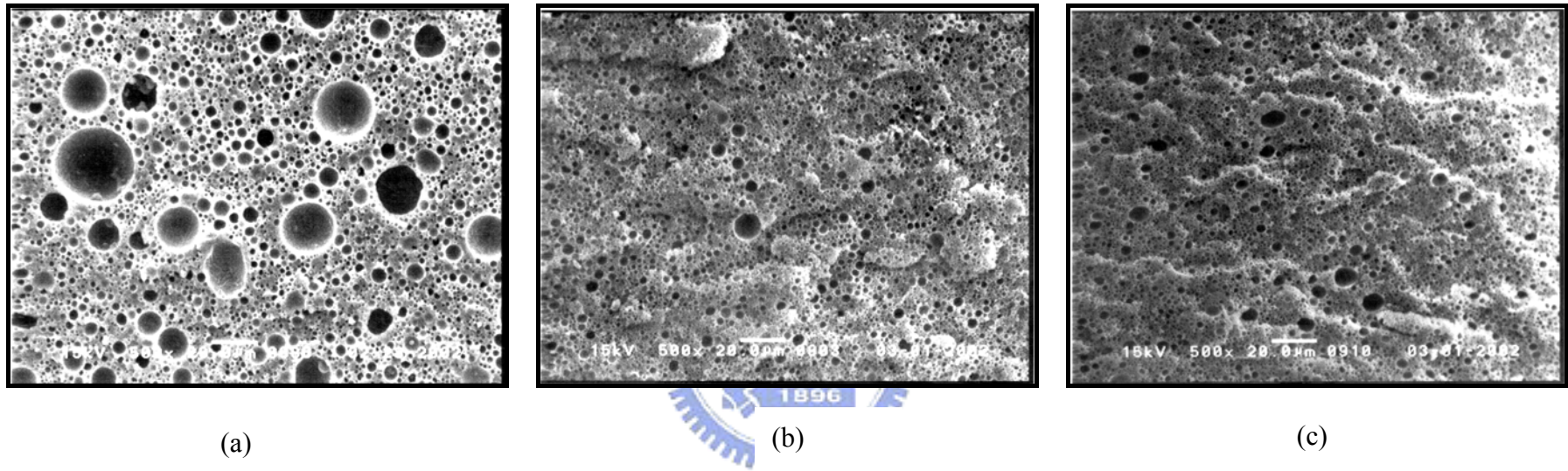
Figure 3-2. SEM micrographs of cryogenic fractured surfaces for various PA-6,6/PPE blends(×500), (a) PA-6,6/PPE = 50/50, (b)

PA-6,6/PPE/Epon828=50/50/1phr (c) PA-6,6/PPE/lmw PPE =50/30/20.

79
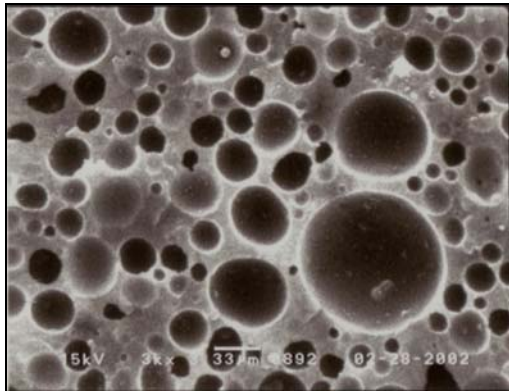
(a)
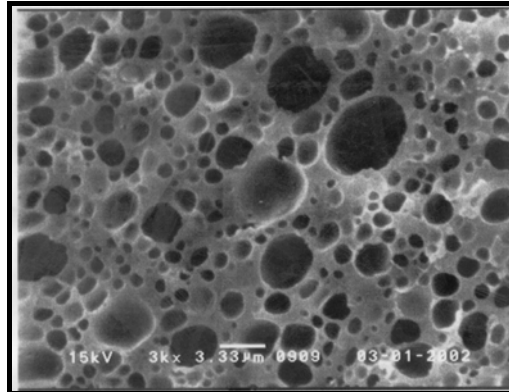
(b)
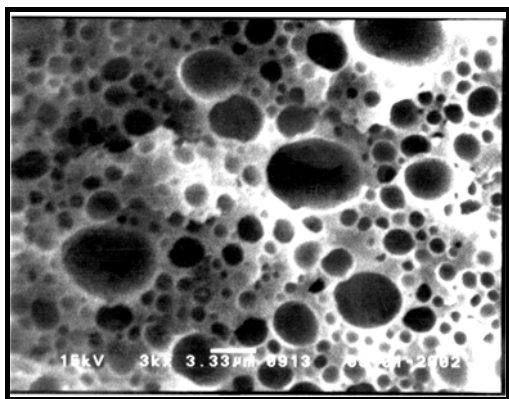
(c)
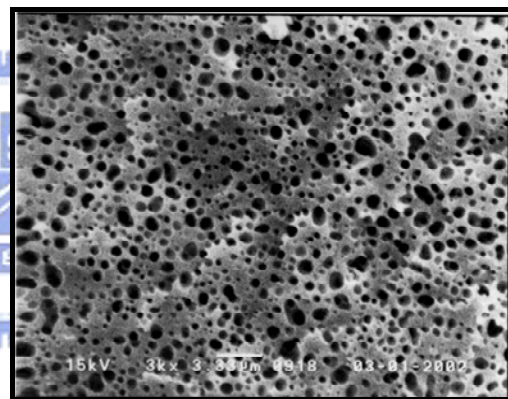
(d)

Figure 3-3. SEM micrographs of cryogenic fractured surfaces for various PA-6,6/PPE blends(×3000): (a) PA-6,6/PPE = 50/50, (b) PA-6,6/PPE/Epon828 = 50/50/1phr, (c) PA-6,6/PPE/lmw PPE/Epon828 = 50/30/20, (d) PA-6,6/PPE/lmw PPE/Epon828 = 50/30/20/1phr.
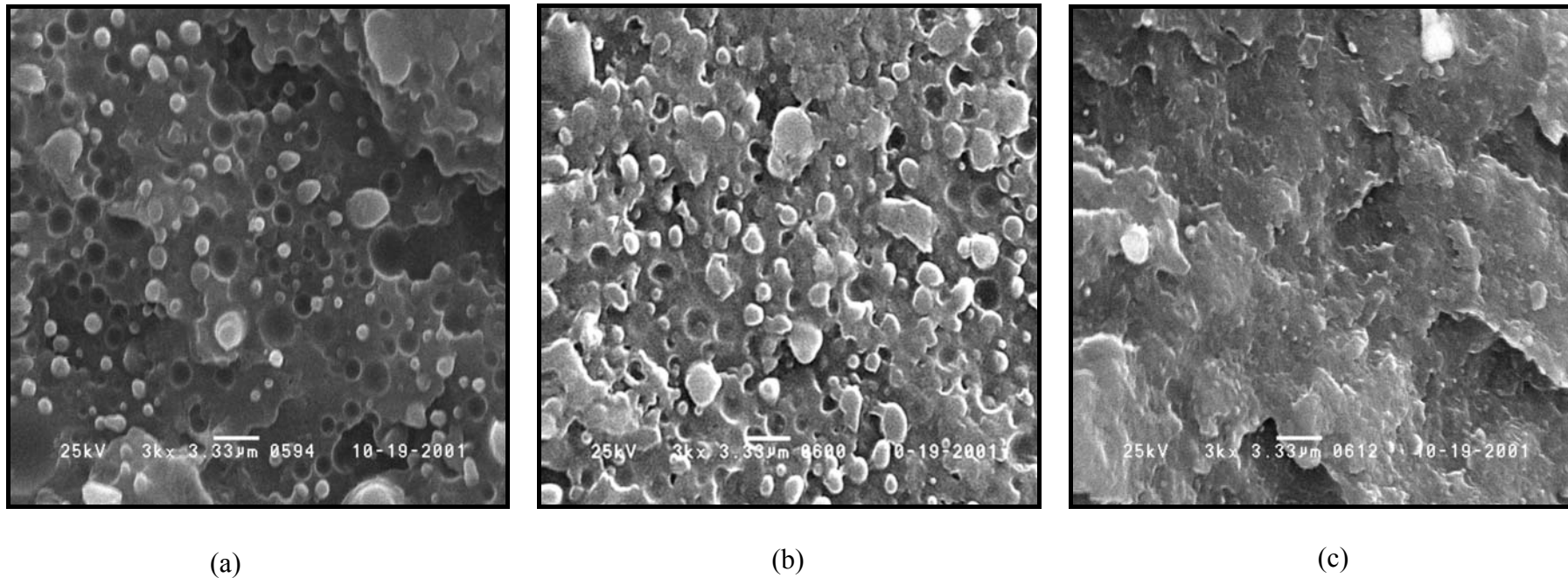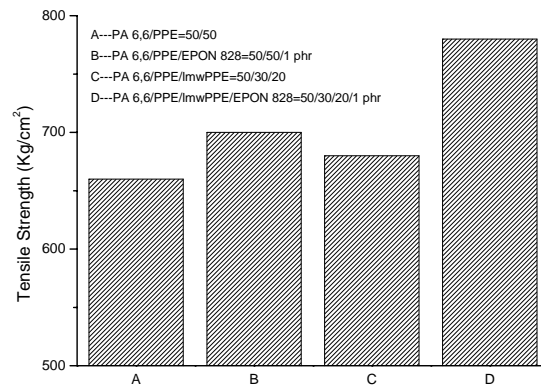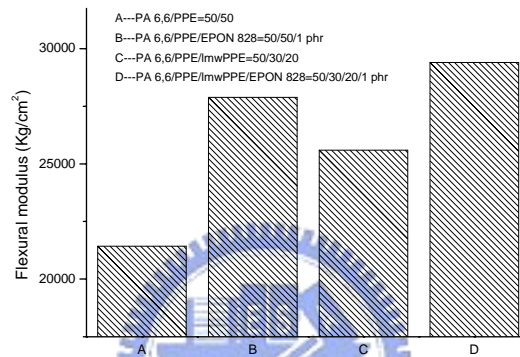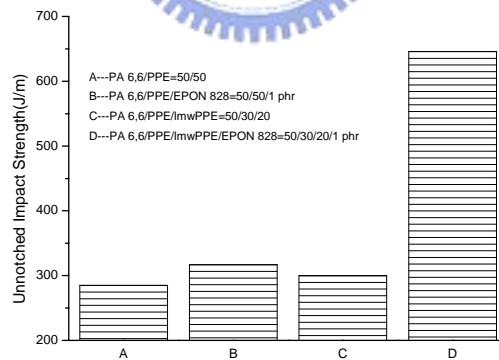
Figure 3-4. SEM micrographs of fractured surfaces for various PA-6,6/PPE blends(×3000) at room temperature: (a) PA-6,6/PPE = 50/50, (b)

PA-6,6/PPE/Epon828 = 50/50/1phr, (c) PA-6,6/PPE/lmw PPE/Epon828 = 50/30/20/1phr.

(A)

(B)

(C)

Figure 3-5. Mechanical properties of various PA 6,6/PPE blends: (A) Tensile strength (B) Flexural modulus, (C) Unnotched impact strength.